

Hot Ductility of High-Mn Steel with Niobium and Titanium

Marek Opiela^{1*}, Gabriela Fojt-Dymara²

¹ Faculty of Mechanical Engineering, Department of Engineering Materials and Biomaterials, Silesian University of Technology, Konarskiego Street 18A, 44-100 Gliwice, Poland

² Faculty of Mechanical Engineering, Department of Engineering Processes Automation and Integrated Manufacturing Systems, Silesian University of Technology, Konarskiego Street 18A, 44-100 Gliwice, Poland

* Corresponding author's e-mail: marek.opiela@polsl.pl

ABSTRACT

The work presents the results of research on the effect of deformation parameters on hot ductility of high-Mn austenitic steel with niobium and titanium. The investigations were carried out on steel with 0.05% C, 24% Mn, 3.5% Si, 1.5% Al, 0.030% Nb and 0.075% Ti. Hot static tensile test was performed using Gleeble 3800 thermomechanical simulator. Samples were deformed in a temperature range from 1050 °C to 1200 °C with a strain rate of $3 \cdot 10^{-3} \text{ s}^{-1}$. The reduction in area (RA), determined in the static tensile test, was the basis for determining the hot ductility of the examined steel. Reduction in area of examined steel decreases from 88% at the temperature of 1050 °C to 59% at 1200 °C. High hot ductility of the investigated steel is the result of the synergy of chemical composition optimization, properly conducted modification of non-metallic inclusions and formed fine-grained microstructure of dynamically recrystallized austenite. In addition to hot ductility, parameters characterizing susceptibility of studied steel to high temperature cracking were also defined, namely: ductility recovery temperature (DRT), nil ductility temperature (NDT) and nil strength temperature (NST) were determined. The values of these temperatures are 1240 °C, 1250 °C and 1270 °C, respectively. This means that the temperature of the beginning of plastic deformation of ingots of this steel may be equal even slightly above 1200 °C. In addition, the high-temperature brittleness range (HTBR) was determined, which is equal 30 °C.

Keywords: high-Mn steel, TWIP-type steel, hot ductility, high-temperature brittleness.

INTRODUCTION

The increasingly higher requirements set by the automotive industry with regards to reducing fuel consumption and emission of harmful exhaust gas, and improving the safety of car users, force the development of new steel grades, characterized by high ductility, significant strength and reduced weight in particular [1, 2]. One of such steel grades, meeting mentioned demands and properties, are austenitic high-manganese steels [3–5]. These steels most often consist of 0.02% to 0.65% C, 15% to 30% Mn and Al and Si with various concentrations [6–9], in some cases also Cr or microadditions Nb and Ti [10–11]. Gradual course of strain induced martensitic transformation [12–14] and/or mechanical twinning [15–18]

guarantees obtaining a particularly good combination of high strength and plasticity ($YS_{0.2} = 250/450 \text{ MPa}$; $UTS = 600/900 \text{ MPa}$; $UEI = 40/80\%$). Moreover, these steels are characterized by high energy absorbing capacity, significantly higher when comparing to conventional steels, and possibility to form complex shaped parts [19, 20]. First results, indicating very advantageous set of properties of TWIP (Twinning Induced Plasticity) steels, were published by Grässel and Frommeyer [21]. They revealed that strengthening of these steels, as a result of mechanical twinning mechanism, leads to obtaining most advantageous combination of strength and plasticity when the concentration of Mn ranges from 20% to 30%, Al from 3% to 5%, and C content – is below 0.6%. In [22], the research was undertaken

to demonstrate the impact of strain rate during dynamic tension (at the rate corresponding to road collision) on mechanical properties of 25Mn-5Al TWIP-type steel. It was revealed that increasing the strain rate from 10^{-4} s^{-1} to 10^3 s^{-1} resulted in increase in $YS_{0.2}$ from approximately 300 MPa to about 550 MPa and increase in UTS from about 500 MPa to about 950 MPa. Despite many advantages of this group of steel and long time since high-manganese steels have been developed, the use of these steels in car production is still minor. Difficulties related to production and processing of high-manganese steels hinder their wider use. The analysis of literature references allows to state that constantly low application of these steels in the automotive industry is caused by the necessity to modify conventional metallurgical processes as well as to deepen the knowledge of their characteristic properties during melting, casting and processing [23, 24]. Very often, these steels demonstrate no sufficient hot ductility necessary for proper implementation of the manufacturing process, taking into consideration its efficiency and costs criteria. It mostly concerns the stages of initial reduction – reducing cross-section of an ingot at the exit from continuous casting mould, ingot straightening operations and the stage of rolling. Low hot ductility of high-manganese steels leads to formation of transverse cracks near the edges of the sheet [25, 26]. Formed defects require cutting metal sheets to obtain high quality products. At the same time, they considerably decrease efficiency and lead to increase of production costs. The cause of crack formation is the presence of precipitations of brittle phases or thin ferrite layer on austenite grains boundaries, high segregation of P and S atoms and non-metallic inclusions, MnS-AlN and AlN-type in particular [27–30]. Mentioned microstructure phase constituents weaken austenite grain boundaries and decrease hot ductility of high-manganese steels and their high-temperature embrittlement [31, 32].

The development of high-manganese steels, their implementation into industrial production and use as constructional materials, is conditioned by the improvement of their ductility, especially at the temperature of hot working, but also at the temperature corresponding to the process of initial cross-section reduction of an ingot after exiting continuous casting mould. Obtaining particularly good combination of strength and plastic properties, as well as guaranteed hot ductility, is possible by appropriate selection of chemical

composition of steel, grain refinement and the use of proper thermo-mechanical treatment [33–35].

The aim of this work is to evaluate hot ductility and susceptibility to high-temperature cracking of newly developed high-Mn steel with niobium and titanium. Achieving the aim of the work required conducting hot static tensile test, microstructure research and X-ray phase analysis.

MATERIALS AND METHODS

The subject of the research was high-Mn austenitic steel, containing 0.05% C, 24% Mn, 3.5% Si, 1.5% Al, and 0.030% Nb and 0.075% Ti. Tested steel has a limited concentration of impurities (0.004% P and 0.015% S) and gases (38 ppm N and 6 ppm O). Test melt, weighing 25.8 kg, was done in VSG-100S type vacuum induction furnace. A mixture of rare earth metals (0.056% Ce, 0.030% La, 0.022% Nd) was used to modify of non-metallic inclusions, introducing it in an amount of 8 g per 1 kg of steel as the last addition to the metal bath. After initial forging (heating temperature 1200 °C; range of forging temperature 1150 ÷ 900 °C), the ingot was rolled on the LPS single-stand reversing mill at the Łukasiewicz Research Network – Institute for Ferrous Metallurgy in Gliwice. The strip was rolled in four passes in the temperature range of 1050 ÷ 900 °C into a 6.5 mm thick sheet. Specimens for testing were taken from the obtained sheet (Fig.1).

In order to evaluate hot ductility, high-temperature tensile tests were conducted using the Gleeble 3800 thermomechanical simulator. Samples were heated at the temperature of 1200 °C for 120 s and then cooled at the rate of 5 °C/s to the set plastic strain temperature and isothermally heated for 30 s prior to deformation. Tensile test was performed in the temperature range from 1050 °C to 1200 °C at the rate of $3 \cdot 10^{-3} \text{ s}^{-1}$. Additionally, one of the specimens was subjected to tension at the austenitizing temperature, i.e. 1200 °C after heating for 30 s. Static hot tensile test was done on samples recommended by Gleeble ($\phi 6 \text{ mm} \times 116.5 \text{ mm}$).

The value of nil strength temperature (NST) was defined during the experiment, consisting in heating the sample to the temperature of 1200 °C at the rate of 20 °C/s, and after exceeding this temperature – at the rate of 1 °C/s until fracture. During the experiment, the sample with a diameter of 6 mm and length of 81 mm was

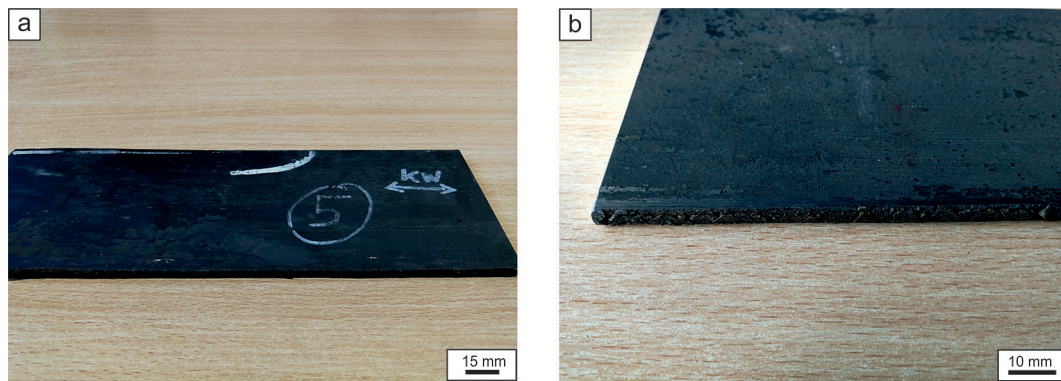


Figure 1. Sections of the examined steel sheets

impacted by tensile force of 80 N [36, 37]. The nil ductility temperature (NDT) and ductility recovery temperature (DRT) were evaluated according to the scheme presented in Figure 2a and Figure 2b, respectively. The T_d marked in Figure 2a – in line with the recommendations, corresponds to the temperature 10 °C lower than the determined NST.

The research of microstructure was performed using light and scanning electron microscopy. In order to reveal microstructure, prepared metallographic specimens were etched in 4% nital or aqua regia (the mixture of concentrated HCl and HNO₃ in 3:1 volume ratio). Microstructure observations were done using LEICA MEF Z1m light microscope from ZEISS, with magnifications ranging from 50x to 500x. Grain size measurements were carried out using the secant method [38], supported by the AXIO Vision image analysis computer program. Morphological details of structural constituents and examination of fracture surfaces after tension were carried out in ZEISS Supra 35 scanning electron microscope. The X-ray phase analysis was performed using

the Panalytical X’Pert PRO X-ray diffractometer, applying cobalt anode lamp, operating at the voltage of 40 kV and current intensity of 30 mA. The register was made in a stepwise manner, recording every 0.05°, as a function of the 2 Θ angle in a range from 20° to 100° and with 50 s counting time. Qualitative X-ray phase analysis was performed in the Bragg-Brentano system with the use of the Xcelerator strip detector.

RESULTS

Performed hot tensile tests allowed to determine the effect of strain temperature (from 1050 °C to 1200 °C) on the form of stress-strain curves of the examined steel (Fig. 3a). The course of stress-strain curves, determined in this Figure, is typical for high-manganese steels [25, 39–41]. The ϵ_{max} marked on the curves – corresponding to the maximum value of yield stress – increase with decreasing test temperature and “shift” to the right, towards larger strains. In the tensile temperature range from 1200 °C to 1050 °C, strength

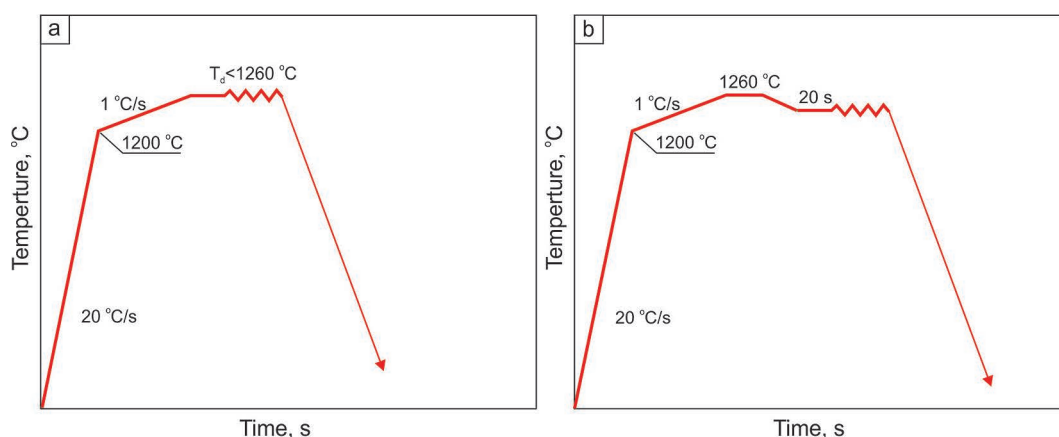


Figure 2. Scheme allowing to determine NDT (a) and DRT (b) of the investigated steel

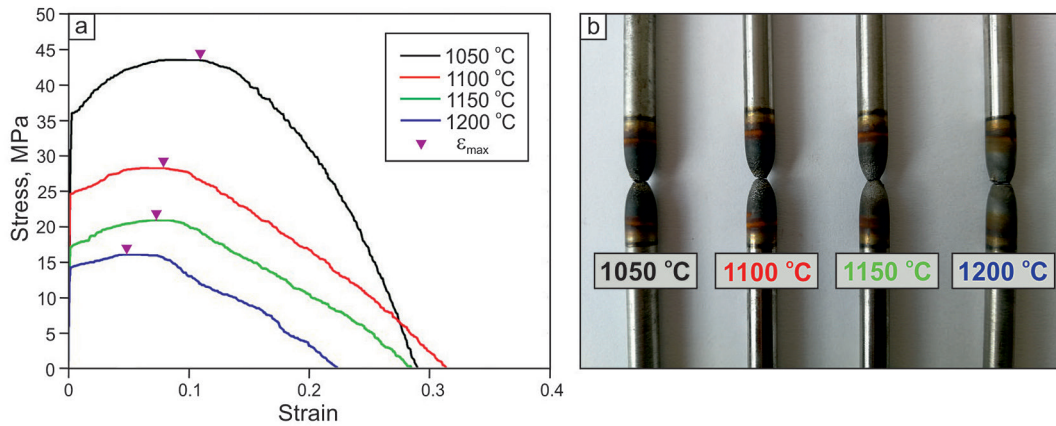


Figure 3. Effect of the temperature of plastic deformation on the shape of tensile curves (a); view of samples after the experiment (b)

of the examined steel increased from approx. 15 MPa to about 43 MPa. In the same temperature range, the ϵ_{max} value increased from approximately 0.045 to about 0.120.

With the aim to evaluate hot ductility of investigated high-Mn steel with niobium and titanium, the reduction in area was determined after tensile test. Results of the effect of temperature of plastic deformation on the reduction in area are shown in Figure 4. The data presented in this figure are the arithmetic mean of three tests at each of the temperatures. The reduction in area at the temperature of 1050 °C is equal about 89%, at the temperature of 1100 °C about 85%, at the temperature of 1150 °C approx. 76%, and at the temperature of 1200 °C – approx. 59%. According to the literature reports [42, 43], steels with reduction in area value exceeding 40%

should be used in order to avoid cracks formation during initial reduction of the continuous ingot. High-manganese steel at the highest test temperature, i.e. 1200 °C, demonstrates the reduction in area higher than recommended by approximately 20%, which should be considered satisfactory.

The steel is characterized by low degree of contamination with non-metallic inclusions. Detailed data on the quantitative analysis of non-metallic inclusions in the studied steel are presented in [27]. The presence of non-metallic inclusions, revealed (on longitudinal microsections) near the sample fracture area, is shown in Figure 5. Non-metallic inclusions found in studied high-manganese steel, in most cases, have globular morphology with average diameter not exceeding 1 mm. Most frequently revealed non-metallic inclusions were S(Ce, La, Nd) sulphides.

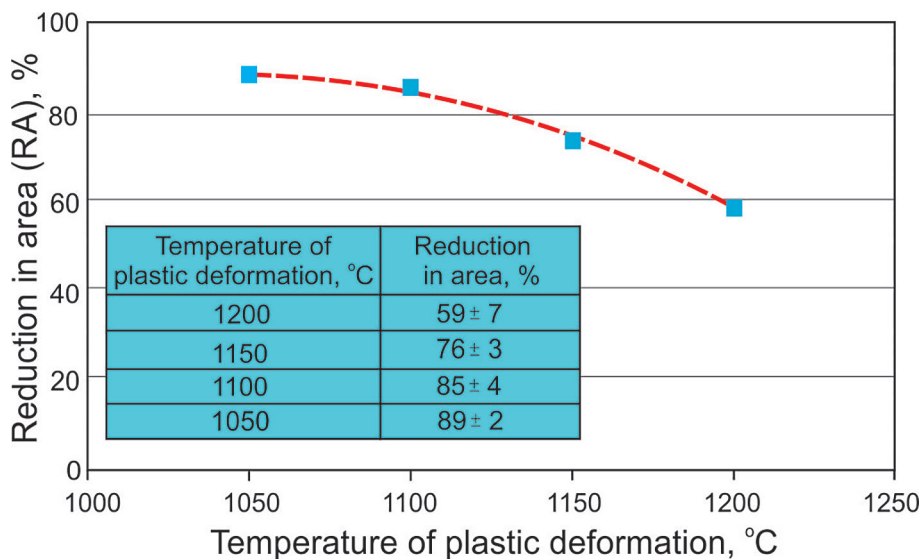


Figure 4. Effect of the temperature of plastic deformation on the reduction in area

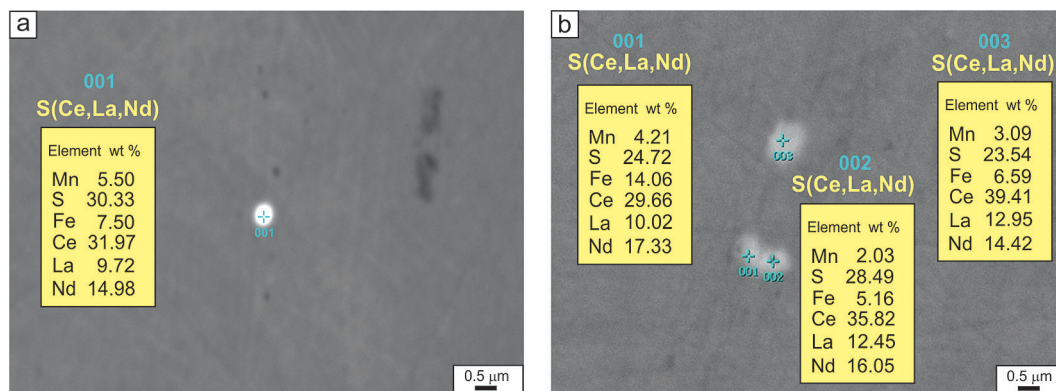


Figure 5. Chemical composition of S(Ce,La,Nd) non-metallic inclusions depending on the plastic deformation temperature: a) 1050 °C, b) 1200 °C

No AlN nitrides harmful to hot ductility or MnS-AlN complex inclusions were revealed in the examined steel [44–46]. The presence of TiN nitrides (Fig. 6) as well as (Ti,Nb)(C,N) carbonitrides was found on the longitudinal microsections – Figure 7. Size of revealed particles ranges from 100 μm to 200 μm. According to the literature reports [47, 48], particles containing Ti and Nb of such sizes will not decrease hot ductility. Diversified microstructure of austenite, revealed over relatively long length of the specimen, plastically deformed at the temperature of 1050 °C, is presented in Figure 8. Grains, elongated in the direction of applied stress, are visible in the vicinity of the fracture, and on their boundaries – very fine recrystallized austenite grains with average diameter of approx. 10 μm. In some of the elongated and flattened austenite grains, laths of the ε martensite were revealed (Fig. 8b, 8c). The presence of this phase in the examined steel is confirmed by peaks appearing

in the X-ray diffraction pattern, deriving from the (010)ε, (200)ε, (110)ε and (210)ε planes – Figure 9.

Completely recrystallized austenite microstructure was noted in the area of the sample, slightly further away from the crack front (Fig. 8a), and the average grain diameter of this phase was equal approx. 25 μm. However, in the area of the sample that does not show the effect of plastic deformation, homogeneous austenite microstructure with twins can be observed (Fig. 8d – on the right). Fine-grained microstructure of recrystallized austenite determines high ductility of analyzed steel at the temperature of 1050 °C (RA = 89%). Similar microstructure, revealed close to the fracture point, was noted in case of the sample plastically deformed at the temperature of 1100 °C (Fig. 10). In the area closest to the fracture, microstructure is composed of elongated and flattened grains of plastically deformed austenite, and small grains of recrystallized γ phase

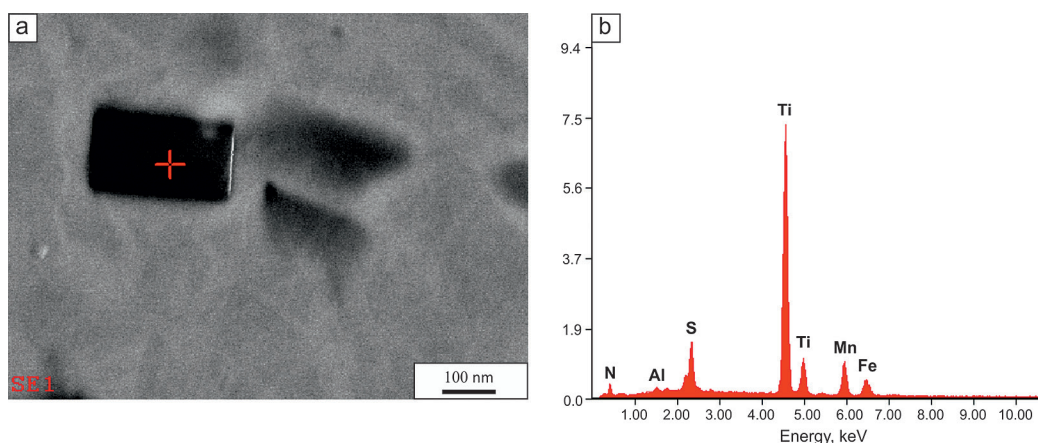


Figure 6. TiN nitride in the steel microstructure: a) image of the particle, b) spectrogram of the precipitation; plastic deformation temperature of 1200 °C

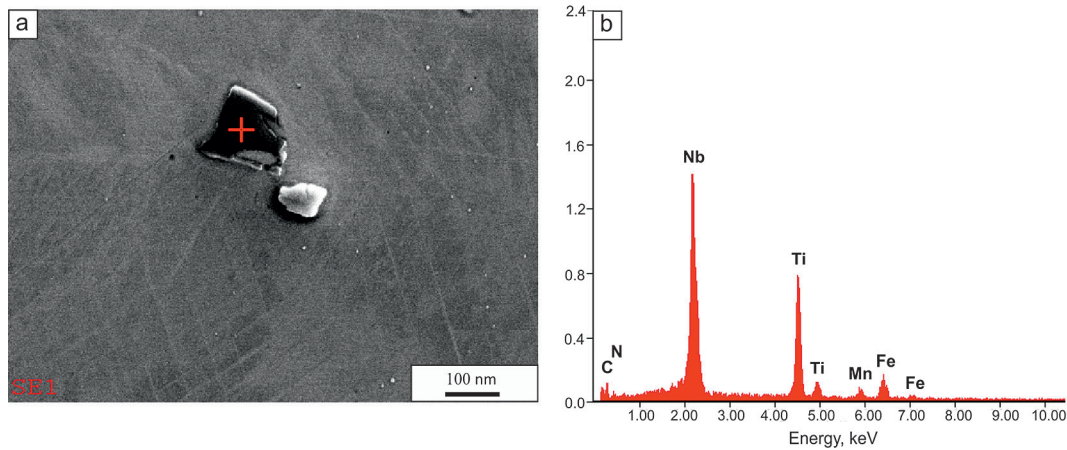


Figure 7. (Ti,Nb)(C,N) carbonitride in the steel microstructure: a) image of the particle, b) spectrogram of the precipitation; plastic deformation temperature of 1100 °C

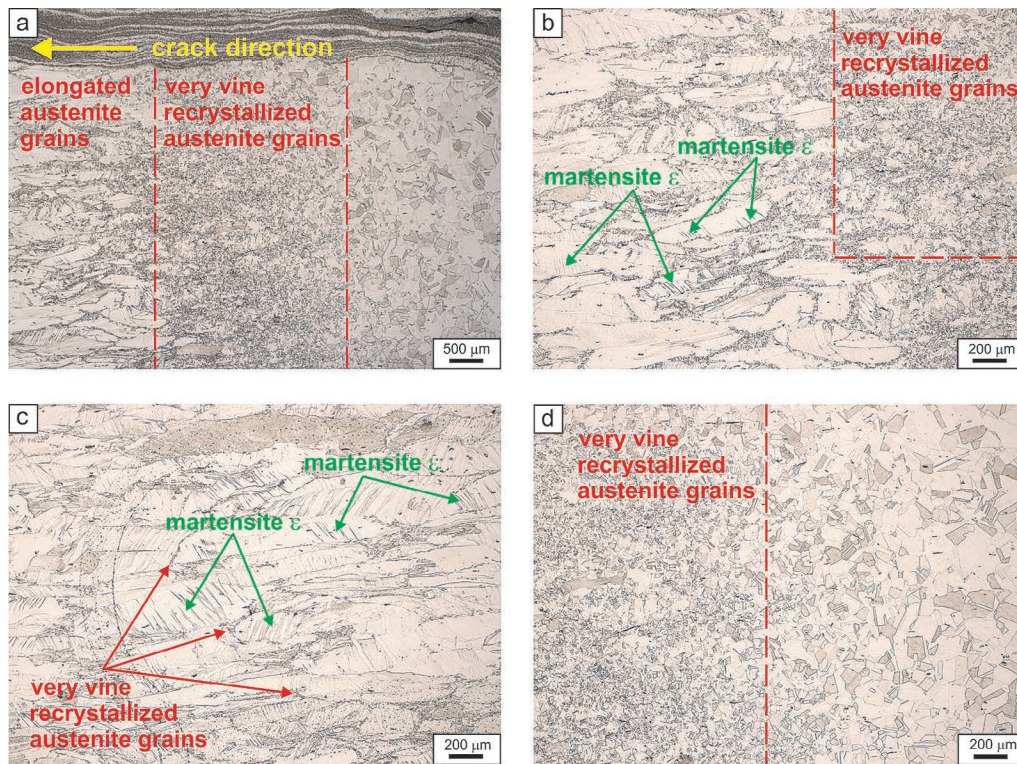


Figure 8. Microstructure of the steel after plastic deformation at the temperature of 1050 °C: a) diversified microstructure of austenite; b, c) elongated austenite grains and very fine grains of recrystallized g phase as well as locally present laths of the ϵ martensite; d) recrystallized austenite (on the left)

are located on their boundaries (Fig. 10a, b). Similarly as in case of the specimen deformed at the temperature of 1050 °C, presence of the ϵ martensite, located in the elongated austenite grains, was also disclosed. Average grain diameter of dynamically recrystallized austenite is equal approx. 46 μm (Fig. 10d). Similar microstructure was revealed in case of samples deformed at the temperature of 1150 °C and 1200 °C. The average diameter of recrystallized austenite grains after plastic

deformation at the temperature of 1150 °C is equal approximately 58 μm, and after austenitizing at the temperature of 1200 °C – approx. 62 μm.

In order to assess susceptibility of studied steel to cracking, high-temperature plasticity characteristics (NST, NDT and DRT) as well as high-temperature brittleness range (HTBR), which corresponds to the difference between NST and DRT [49], were determined. First defined was the nil strength temperature (NST). Obtained NST

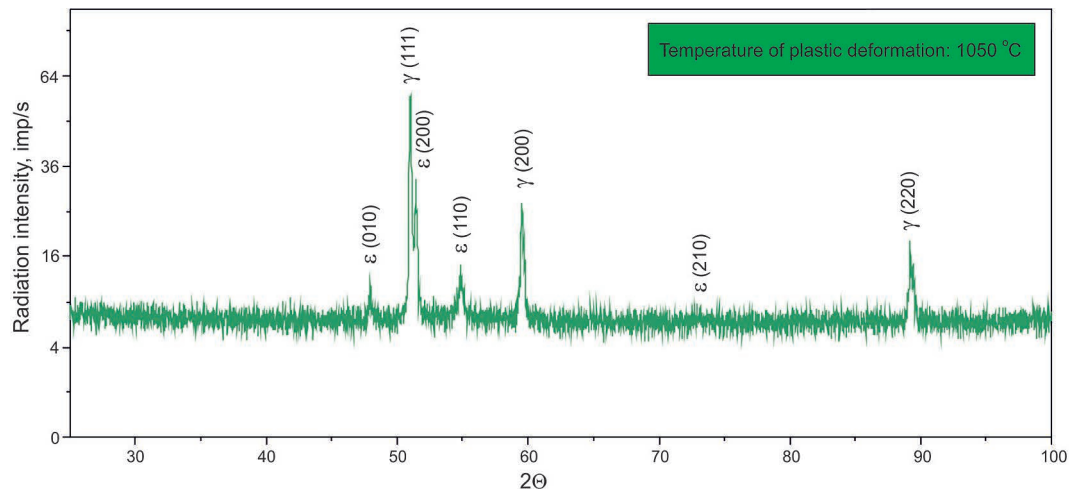


Figure 9. X-ray diffraction pattern of tested steel after plastic deformation at the temperature of 1050 °C

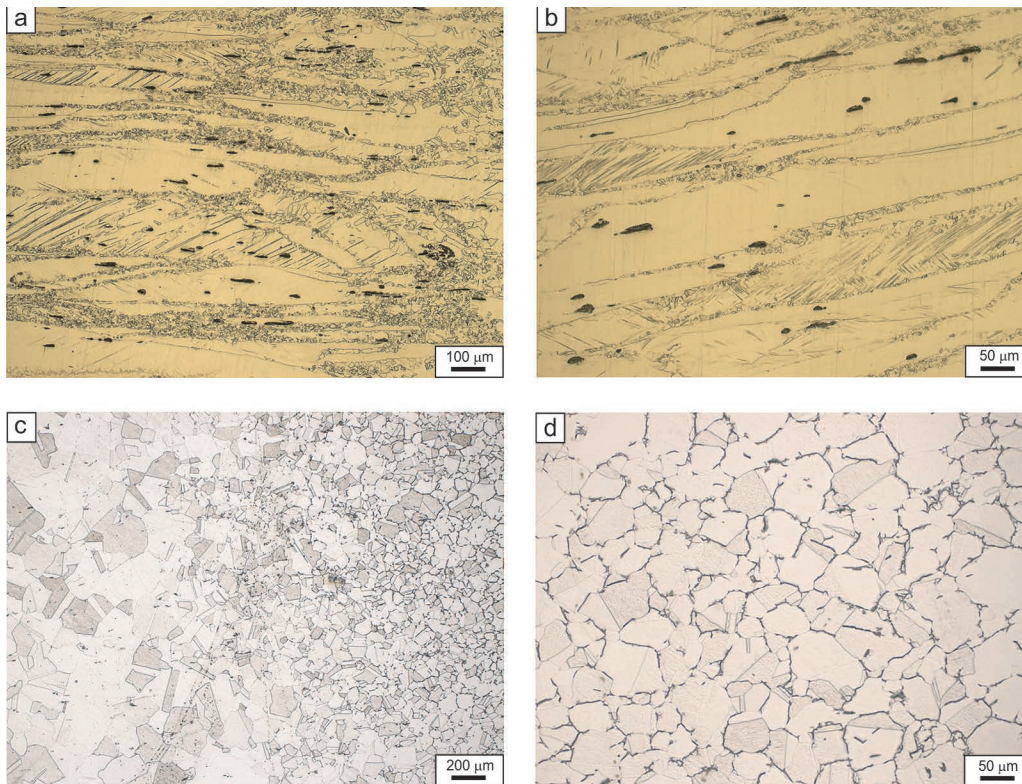


Figure 10. Microstructure of the steel after plastic deformation at the temperature of 1100 °C: a, b) elongated austenite grains and very fine grains of recrystallized γ phase as well as locally present laths of the ϵ martensite; c) recrystallized austenite (on the right); d) enlarged fragment of the right part in Fig. 10c

values correspond to the temperature at which the steel lost its stability. As a result, sharp drop in temperature is visible on the diagram of temperature changes as a function of time (Fig. 11). The average NST value was determined based on three tests performed. For the examined steel with Nb and Ti microadditions it is equal 1270 °C. Fracture of the sample after breaking at the $NST_2 = 1269$ °C is presented in Figure 12. The research

conducted using scanning electron microscope allowed to observe the presence of local partial melting of austenite grain boundaries. Intercrystalline and locally transcrystalline brittle fractures were also disclosed on the fracture surface.

Determined NST value of 1270 °C was the starting point for designing an experiment, enabling evaluation of NDT and DRT (Fig. 2). The effect of plastic deformation temperature on

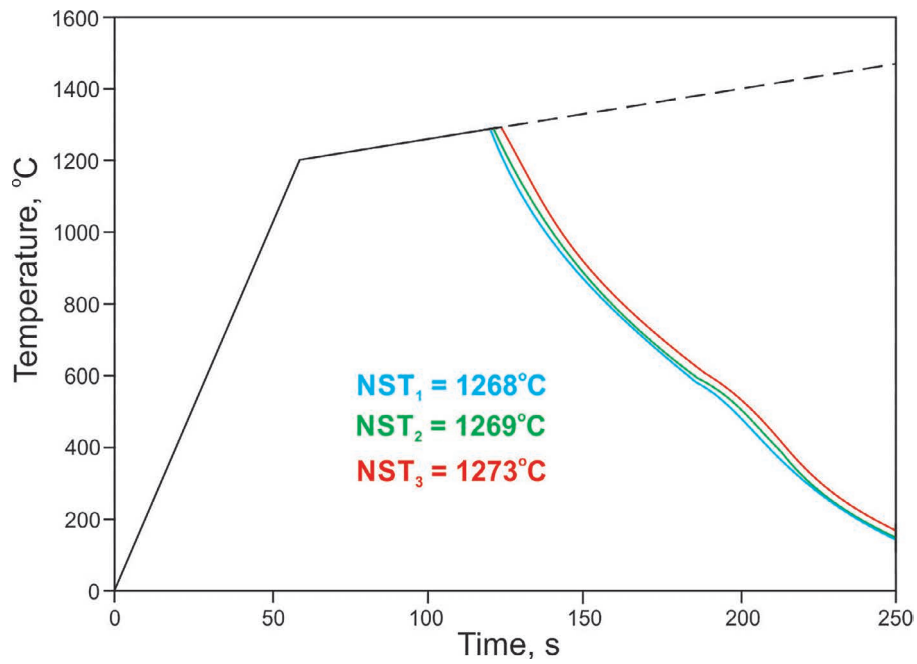


Figure 11. Diagram of temperature changes as a function of time of the tested steel

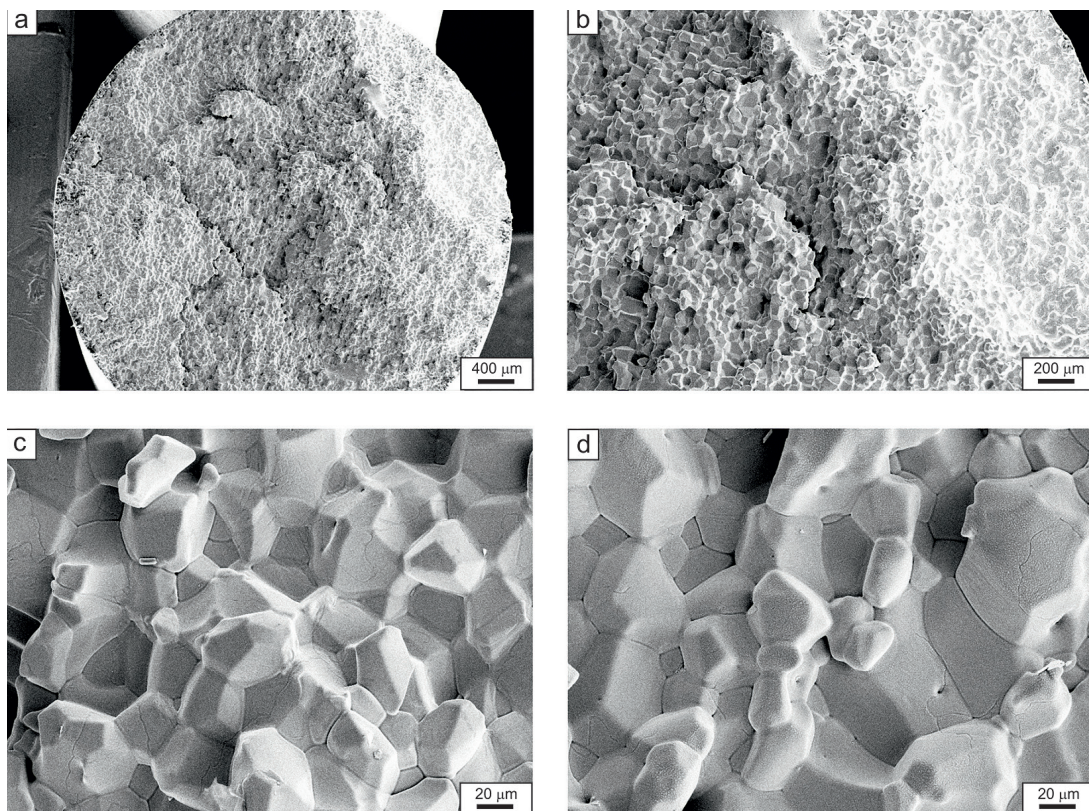


Figure 12. Fracture surface of the specimen after breaking at the temperature of 1269 °C

the reduction in area of tested steel samples is shown in Figure 13. Investigated high-manganese steel demonstrates mild decrease in the reduction in area (from 1200 °C to 1245 °C). In the given temperature range, the reduction in area decreased from approx. 58% to about 3% (RA for

designation NDT) and from about 45% to about 1% (RA for designation DRT). Reduction in area details, which are the arithmetic mean of three tests, given in Figure 13, indicate that the temperature at which examined steel did not show any plasticity is equal 1250 °C (NDT). However, the

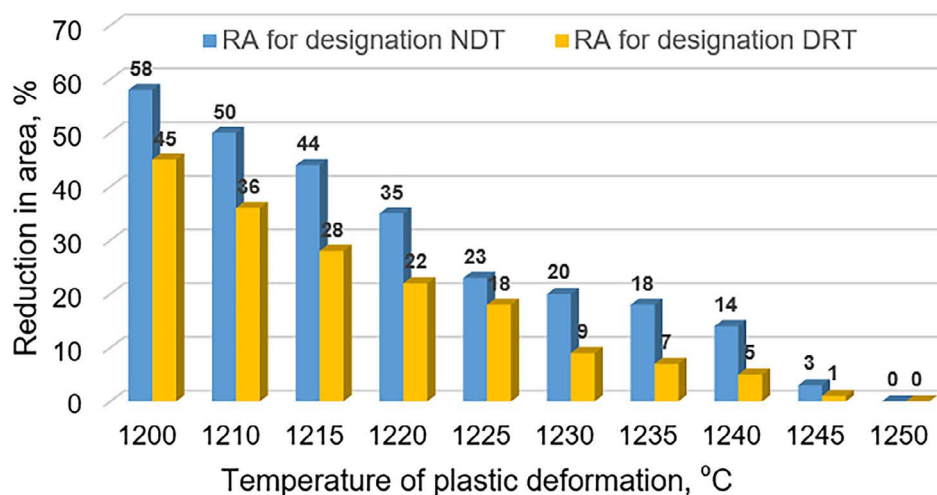


Figure 13. Effect of tensile temperature on the reduction in area of examined steel, obtained from tests performed according to the assumptions set together in Fig. 2a and Fig. 2b

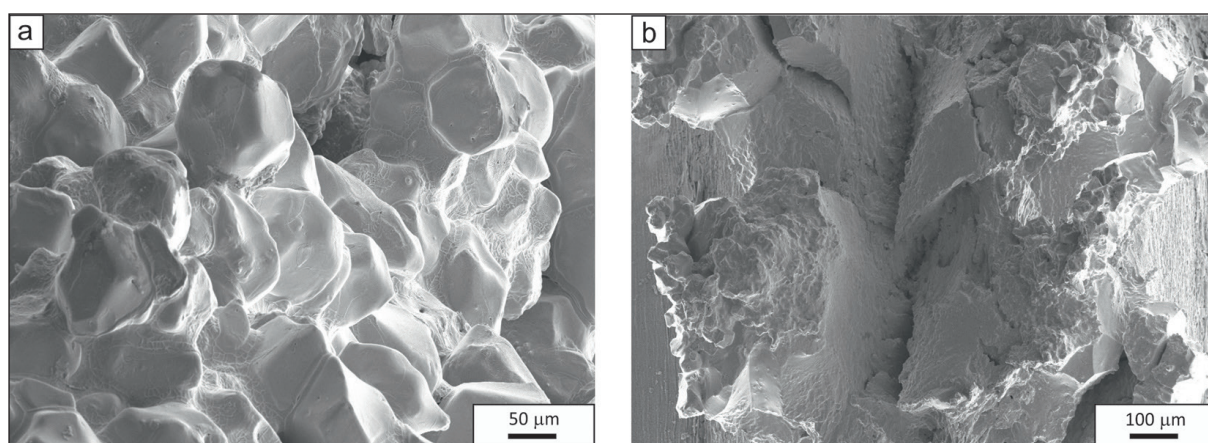


Figure 14. Fracture surface of the specimen after hot tensile tests at the temperature: a) NDT = 1250 °C; b) DRT = 1240 °C

reduction in area of 5% was obtained in case of the sample deformed at the temperature of 1240 °C (DRT). Fractures of samples after tension at the temperature of 1250°C and 1240 °C, are presented in Figure 14a and in Figure 14b, respectively. Local partial melting of grain boundaries and few cracks were noted in case of the sample subjected to tension at the temperature of 1250 °C (Fig. 14a). However, brittle fracture with flat surfaces and locally occurring characteristics of plastic fracture were noted in case of the sample after tension at ductility recovery temperature (Fig. 14b).

DISCUSSION

Customer requirements for steel products, dedicated to the automotive industry, determine the necessity to develop new grades of

high-strength steel. Moreover, modern steels for automotive industry should also be characterized by guaranteed hot ductility – already during the initial reduction cross-section of the continuous ingot and straightening operations. The condition for achieving expected functional properties of products made of high-manganese steels is to correctly select chemical composition, taking into consideration the appropriate proportion of Si and Al and the concentration of Nb and Ti microadditions – responsible for formation of fine-grained austenite microstructure, control of phase transitions occurring in the thermo-mechanical treatment process and after its finish.

The shape and the course of work-hardening curves, obtained in hot static tensile test (Fig. 3a), are typical for high-manganese steels with similar chemical composition [25, 39–40] and indicate that in the tested temperature range, decrease in

strain hardening results from dynamic recrystallization. The reduction in area (RA), defined in the static tensile test, was the basis for determining the hot ductility. The reduction in area of high-Mn steel in the test temperature range, i.e. from 1050 °C to 1200 °C, decreases from approx. 89% to about 59% (Fig.4). The RA value decreasing along with increasing temperature is probably a result of combined effect of increasing average size of recrystallized austenite grains and a larger portion of Ti and Nb microadditions dissolved in the solution. The effect of Nb and Mo concentration on the hot ductility of high-manganese Fe-21Mn-1.3Al-1.5Si-0.5C type steel was investigated in [41]. For instance, the reduction in area for steel, containing 0.5% C, 20.0% Mn, 1.3% Si, 1.5% Al and 0.083% Nb – in temperatures from 700 °C to 1100 °C – ranged from approx. 52% to about 31%. Ductility of steel with 0.6% C, 18% Mn, 0.1% Si, 1.50% Al, 0.075% Ti, 0.032% Nb and 0.0028% B, was examined in the same temperature range. Qaban, Mintz and Kang [50] revealed that the reduction in area of tested steel decreased from approx. 55% at the temperature of 700 °C to about 40% – at the temperature of 1100 °C. Ductility in a slightly wider temperature range (700 °C ÷ 1200 °C) was evaluated in [25, 39]. Steel, containing 0.73%, 22.03% Mn and 0.17% Si, in the examined temperature range, showed the reduction in area ranging from approx. 33% to about 25% [25]. Liu et al. [39] researched steel consisting of 0.66% C, 23.6% Mn and 1.40% Al. In the tensile temperature range from 700 °C to 1200 °C, the reduction in area of the examined steel decreased from approx. 30% to about 8%. Mentioned results, related to hot ductility of high-manganese steels, indicate that obtained values of the reduction in area of newly developed steel with Nb and Ti microadditions, presented in Figure 4, should be considered as promising. The presence of globular, highly dispersive non-metallic inclusions, mainly S(Ce, La, Nd) sulphides, was revealed in the examined steel (Fig. 5). This proves that liquid steel was properly modified with rare earth elements. Non-metallic inclusions, characterized with such morphology, will favour production of rolled products with guaranteed strength and high hot ductility. Non-metallic inclusions of the AlN or Mn-AlN, which decrease hot ductility and cause intergranular embrittlement, were not revealed in the tested steel [50, 51]. In addition to non-metallic inclusions, TiN nitrides (Fig. 6) and (Ti,Nb)(C,N) carbonitrides

(Fig. 7) were revealed in microstructure of examined steel. The size of disclosed particles ranged from 100 µm to 200 µm. Literature data [39, 48, 52, 53] indicate that the presence of this type of particles, smaller than 50 µm, may cause sharp decrease in hot ductility. Fine particles, present in the austenite matrix, increase compressive stress at grain boundaries, facilitating growth and connection of cracks, consequently leading to decrease of ductility [42]. Turkdogan [54] showed that TiN particles of sufficiently large sizes are privileged nucleation areas for NbC carbides. Considering that these phases demonstrate mutual solubility [55, 56], they will form (Ti,Nb)(C,N) complex carbonitrides – which improve ductility. Microstructure of the samples near fracture consists of elongated austenite grains, on the boundaries of which there are very fine grains of recrystallized γ phase (Fig. 8a-c; Fig. 10a-b). In the areas of the sample slightly further away from the fracture area, completely recrystallized austenite microstructure was observed, with average grain diameter increasing from approx. 25 µm to about 62 µm – for samples subjected to tension in the temperature range from 1050 °C to 1200 °C. Hot ductility can be improved by the interaction of recrystallized grains with sufficiently small diameter with micro-cracks, by isolating them from grain boundaries. This mechanism was described in detail by Mintz [57]. In some elongated austenite grains, the ϵ martensite was revealed (Fig. 8b-c; Fig. 10a-b). Such ϵ martensite, with similar morphology, was revealed by Grajcar [58] during the research of high-manganese steel with chemical composition comparable to the analyzed steel.

The defined value of nil strength temperature (NST = 1270 °C) is typical for high-manganese steels. For example, the X60MnAl30-9 steel grade, consisting of 0.62% C, 30% Mn, 0.37% Si and 9% Al, shows NST = 1255 °C [59]. High-manganese steel containing 0.04% C, 27.5% Mn, 4.2% Si, 2.0% Al, and 0.033% Nb shows NST = 1250 °C [49]. Steels with low Mn concentration are characterized by significantly higher NST values. For instance, the S960QL steel grade, containing 0.16% C, 1.24% Mn, 0.22% Si, 0.20% Cr and 0.041% V, demonstrates NST = 1400 °C [37]. While the NST for the X15CrNiSi20-12 austenitic steel grade, consisting of 0.16% C, 1.0% Mn, 1.5% Si, 20.2% Cr and 12.3% Ni, is equal 1359 °C [60]. A similar value of NST = 1369 °C is shown steel consisting of 0.57% C, 0.72% Mn, 0.25% Si, 0.07% Cr and 0.03%

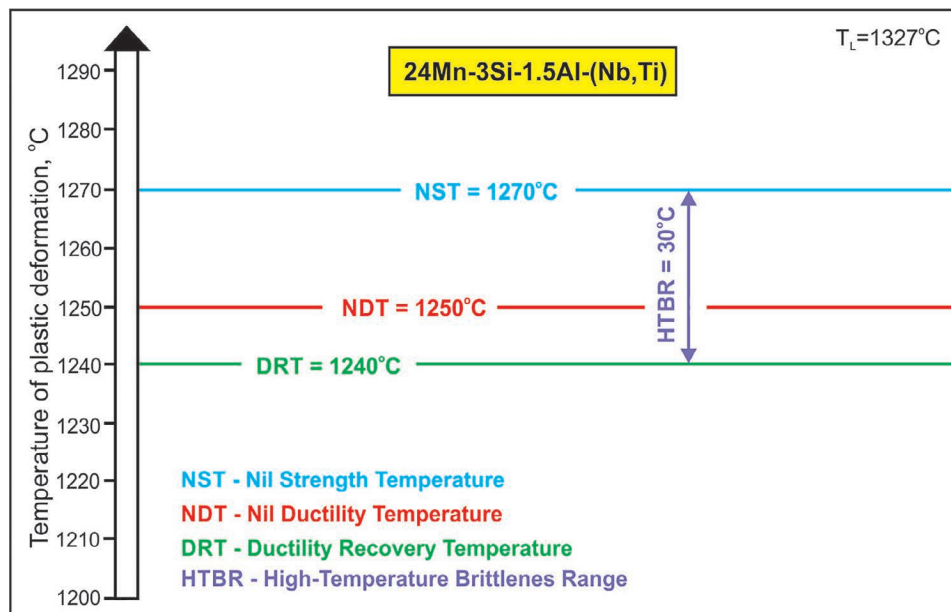


Figure 15. High-temperature plasticity characteristics of studied steel

Ni [36]. High-temperature tensile tests also allowed determining nil ductility temperature (NDT) and ductility recovery temperature (DRT). Defined NDT and DRT values are equal 1250 °C and 1240 °C, respectively. Summary of parameters, characterizing the susceptibility of studied steel to high temperature cracking, is presented in Figure 15. For tested steel, the HTBR is relatively narrow and is equal 3 °C.

CONCLUSIONS

The research, conducted high-Mn steel with niobium and titanium allows to draw the following conclusions: In the temperature range from 1050 °C to 1200 °C, the reduction in area of examined steel decreased from approx. 89% to about 59%. High hot ductility (RA from approx. 89% to about 59%) is the result of combined effect of properly conducted process of modifying non-metallic inclusions and fine-grained microstructure of dynamically recrystallized austenite. Hot ductility can also be improved by microadditions of Nb (0.030%) and Ti (0.075%) introduced into the steel. Microaddition of Ti binds the whole nitrogen into stable TiN nitrides, eliminating the possibility of precipitation of AlN nitrides that are harmful to ductility. However, microaddition of Nb ensures formation of complex (Ti,Nb)(C,N) carbonitrides – which advantageously effect hot ductility. Defined high-temperature plasticity characteristics (NST = 1270 °C, NDT = 1250 °C and DRT = 1240 °C) indicate that the temperature

of the beginning of processing of ingots from tested steel may be equal 1200 °C – with guaranteed ductility at this temperature (RA > 40%). Low HTBR value of 30 °C indicates low susceptibility of the examined steel to hot cracking.

Acknowledgements

The publication is supported by the Rector's pro-quality grant. Silesian University of Technology, grant number 10/010/RGJ23/1138.

REFERENCES

- Bordone M., Monsalve A., Perez Ipina J. Fracture toughness of high-manganese steels with TWIP/TRIP effects. *Engineering Fracture Mechanics* 2022; 275(108837): 1–15. doi: 10.1016/j.engfracmech.2022.108837.
- Ma H., Chen Ch., Li J., Wang X., Qi X., Zhang F., Tang T. Effect of pre-deformation degree on tensile properties of high carbon high manganese steel at different strain rates. *Materials Science and Engineering A* 2022; 829(142146): 1–12. doi: 10.1016/j.msea.2021.142146.
- Wang Y., Yu H., Ma Z., Mu R., Song R., Taylor T. Room temperature compression deformation behavior of a Cr-Nb alloyed high manganese steel. *Vacuum* 2023; 207(111696): 1–8. doi: 10.1016/j.vacuum.2022.111.696.
- Lee S., Lee S-Y., Han J., Hwang B. Deformation behavior and tensile properties of an austenitic Fe-24Mn-4Cr-0.5C high-manganese steel: Effect of grain

- size. *Materials Science and Engineering A* 2019; 742: 334–343. doi: 10.1016/j.msea.2018.10.107.
5. Song D., Beier H.T., Vormwald M. The effect of loading direction and pre-deformation on the low-cycle fatigue behavior of high-manganese twinning-induced plasticity steels. *International Journal of Fatigue* 2022; 174(107737): 1–14. doi: 10.1016/j.ijfatigue.2023.107737.
 6. Choi W.S., Sandlöbes S., Malyar N.V., Kirchlechner C., Korte-Korzel S., Dehm G., Choi P., Raabe D. On the nature of twin boundary-associated strengthening in Fe-Mn-C steel. *Scripta Materialia* 2018; 156: 27–31. doi: 10.1016/j.scriptamat.2108.07.009.
 7. Madivala M., Schwedt A., Prahl U., Bleck W. Strain hardening, damage and fracture behavior of Al-added high Mn TWIP steels. *Metals* 2019; 9(367): 1–24. doi: 10.3390/met9030367.
 8. Pierce D.T., Jiménez J.A., Bentley J., Raabe D., Witting J.E. The influence of stacking fault energy on the microstructural and strain-hardening evolution of Fe-Mn-Al-Si steels during tensile deformation. *Scripta Materialia* 2015; 100: 178–190. doi: 10.1016/j.actamat.2015.08.030.
 9. Opiela M., Fojt-Dymara G., Grajcar A., Borek W. Effect of grain size on the microstructure and strain hardening behavior of solution heat-treated low-C high-Mn steel. *Materials* 2020; 13(7): 1–13. doi: 10.3390/ma14123254.
 10. Fu H., Zhang W., Zhang T., Huang X., Chen P., Wu H., Li Z., Shan Q. MC precipitates affected by nitrogen addition in Ti-V-Nb micro-alloyed high manganese steel. *Materials Today* 2023; 37(107089): 1–15. doi: 10.1016/mtcomm.2023.107089.
 11. Grajcar A., Kozłowska A., Topolska S., Morawiec M. Effect of deformation temperature on microstructure evolution and mechanical properties of low-carbon high-Mn steel. *Advances in Materials Science and Engineering* 2018; 7369827: 1–7. doi: 10.1155/2018/7369827.
 12. Li X., Chen L., Zhao Y., Misra R.D.K. Influence of manganese content on ϵ - α -martensitic transformation tensile properties of low-C high-Mn TRIP steels. *Materials and Design* 2018; 142: 190–202. doi: 10.1016/j.matdes.2018.01.026.
 13. An D., Zaefferer S. Formation mechanism of dislocation patterns under low cycle fatigue of a high-manganese austenitic TRIP steels with dominating planar slip mode. *International Journal of Plasticity* 2019; 121: 244–260. doi: 10.1016/j.ijplas.2019.06.009.
 14. Kaar S., Schneider R., Križan D., Béal C., Sommitsch C. Influence of quenching and partitioning process on the transformation kinetics and hardness in a lean medium manganese TRIP steel. *Metals* 2019; 9(353): 1–13. doi: 10.3390/met9030353.
 15. De Cooman B.C., Estrin Y., Kim S.K. Twinning-induced plasticity (TWIP) steels. *Acta Materialia* 2018; 142: 283–362. doi: 10.1016/j.actamat.2017.06.046.
 16. Radwański K., Kuziak R., Rozmus R. Structure and mechanical properties of dual-phase steel following heat treatment simulations reproducing a continuous annealing line. *Archives of Civil and Mechanical Engineering* 2019; 19: 453–468. doi: 10.1016/j.acme.2018.12.006.
 17. Sevsek S., Haase C., Bleck W. Strain-rate-dependent deformation behavior and mechanical properties of a multi-phase medium-manganese steel. *Metals* 2019; 9(344): 1–20. doi: 10.3390/met9030344.
 18. Grajcar A., Opiela M., Fojt-Dymara G. The influence of hot-working conditions on a structure of high-manganese steel. *Archives of Civil and Mechanical Engineering* 2009; 19(3): 49–58. doi: 10.1016/S1644-9665(12)60217-9.
 19. Kim J.K., De Cooman B.C. Stacking fault energy and deformation mechanisms in Fe-xMn-0.6C-yAl TWIP steel. *Materials Science and Engineering A* 2016; 676: 216–231. doi: 10.1016/j.msea.2016.08.106.
 20. Wesselmecking S., Haupt M., Ma Y., Song W., Hirt G., Bleck W. Mechanism-controlled thermomechanical treatment of high manganese steels. *Materials Science and Engineering A* 2021; 828: 1–9. doi: 10.1016/j.msea.2021.142056.
 21. Grässel O., Frommeyer G. Effect of martensitic phase transformation and deformation twinning on mechanical properties of Fe-Mn-Si-Al steels. *Materials Science Technology* 1998; 14(12): 1213–1217. doi: 10.1179/mst.1998.14.12.1213.
 22. Jabłońska M., Niewiński G., Kawalla R. High manganese steel TWIP – technological plasticity and selected properties. *Solid State Phenomena* 2014; 212: 87–90. doi: 10.4028/www.scientific.net/SSP.212.87.
 23. Shen Y.F., Jia N., Misra R.D.K., Zu L. Softening behavior by excessive twinning and adiabatic heating at high strain rate in a Fe-20Mn-0.6C TWIP steel. *Acta Materialia* 2016; 103: 229–242. doi: 10.1016/j.actamat.2015.09.061.
 24. Chen Y., Liu G.M., Li H.Y., Zhang X.M., Ding H. Microstructure, strain hardening behavior, segregation and corrosion resistance of an electron beam welded thick high-Mn TWIP steel plate. *Journal of Materials Research and Technology* 2023; 25: 1105–1114. doi: 10.1016/j.jmrt.2023.06.010.
 25. Lan P., Tang H.Y., Zhang J.Y. Hot ductility of high alloy Fe-Mn-C austenite TWIP steel. *Materials Science and Engineering A* 2016; 660: 127–138. doi: 10.1016/j.msea.2016.02.086.
 26. Wang S.H., Liu Z.Y., Zhang W.N., Wang G.D., Liu J.L., Liang G.F. Microstructure and mechanical property of strip in Fe-23Mn-3Si-3Al TWIP steel by twin roll casting. *ISIJ International* 2009; 49: 1340–1346. doi: 10.2355/isijinternational.49.1340.

27. Opiela M., Fojt-Dymara G. Effect of non-metallic inclusions on the hot ductility of high-Mn steels. *Advances in Science and Technology. Research Journal* 2023; 17(3): 19-30. doi: 10.12913/22998624/162702.
28. Chu J., Zhang L., Yang J., Bao Y., Ali N., Zhang C. Characterization of precipitation, evolution, and growth of MnS inclusions in medium/high manganese steel during solidification process. *Materials Characterization* 2022; 194(112367): 1–14. doi: 10.1016/j.matchar.2022.112367.
29. Kang S.E., Banerjee J.R., Mintz B. Influence of S and AlN on hot ductility of high Al, TWIP steels. *Materials Science and Technology* 2012; 28: 589–596. doi: 10.1179/1743284711Y.0000000109.
30. Chu J., Nian Y., Zhang L., Bao Y., Ali N., Zhang C., Zhou H. Formation, evolution and remove behavior of manganese-containing inclusions in medium/high manganese steels. *Journal of Materials Research and Technology* 2023; 22: 1505–1521. doi: 10.1016/j.jmrt. 2022.12.023.
31. Han K., Yoo Y., Lee B., Han I., Lee C. Hot ductility and hot cracking susceptibility of Ti-modified austenitic high Mn weld HAZ. *Materials Chemistry and Physics* 2016; 184: 118–129. doi: 10.1016/j.matchemphys.2016.09.032.
32. Kang S.E., Banerjee J.R., Tuling A. Influence of P and N on hot ductility of high Al, boron containing TWIP steels. *Materials Science and Technology* 2014; 30: 1328–1335. doi: 10.1179/1743284714Y.0000000.
33. Sozańska-Jędrusik L., Mazurkiewicz J., Borek W., Matus K., Chmiela B., Zubko M. Effect of Nb and Ti micro-additives and thermo-mechanical treatment of high-manganese steels with aluminum and silicon on their microstructure and mechanical properties. *Archives of Metallurgy and Materials* 2019; 64(1): 133–142. doi: 10.24425/amm.2019.126229.
34. Dobrzański L.A., Borek W., Mazurkiewicz J. Mechanical properties of high-Mn austenitic steel tested under static and dynamic conditions. *Archives of Metallurgy and Materials* 2016; 61(2): 725–730. doi: 10.1515/amm-2016-0124.
35. Yuan X., Chen L., Zhao Y., Di H., Zhu F. Influence of annealing temperature on mechanical properties and microstructures of a high manganese austenitic steel. *Journal of Materials Processing Technology* 2015; 217: 278–285. doi: 10.1016/j.jmatprotec.2014.11.027.
36. Kawulok P., Schindler I., Smetana B., Moravec J., Mertová A., Drozdová M., Kawulok R., Opéla P., Ruzs S. The relationship between nil-strength temperature, zero strength temperature and solid temperature of carbon steels. *Metals* 2019; 10(399): 1–14. doi: 10.3390/met10030399.
37. Kuzsella L., Lukás J., Szűcs K. Nil-strength temperature and hot tensile tests on S960QL high-strength low-alloy steel. *Production Processes and Systems* 2013; 6(1): 67–78. doi: 10.13140/2.1.4655.9369.
38. ASTM E112-10. Standard Test Methods for Determining Average Grain Size. 2004.
39. Liu H., Liu J., Wu B., Shen Y., He Y., Su X. Effect of Mn and Al contents on hot ductility of high alloy Fe-xMn-C-yAl austenite TWIP steels. *Materials Science and Engineering A* 2017; 708: 360–374. doi: 10.1016/j.msea.2017.10.001.
40. Mejia I., Salas-Reyes A.E., Calvo J., Cabrera J.M. Effect Ti and B microadditions on the hot ductility behavior of a high-Mn austenitic Fe-23Mn-1.5Al-1.3Si-0.5C TWIP steel. *Materials Science and Engineering A* 2015; 648: 311–329. doi: 10.1016/j.msea.2015.09.079.
41. Mejia I., Salas-Reyes A.E., Bedolla-Jacuinde A., Calvo J., Cabrera J.M. Effect of Nb and Mo on the hot ductility behavior of a high-manganese austenitic Fe-21Mn-1.3Al-1.5Si-0.5C TWIP steel. *Materials Science and Engineering A* 2014; 616: 229–239. doi: 10.1016/j.msea.2014.08.030.
42. Mintz B., Qaban A. The influence of precipitation, high levels of Al, Si, P and small B addition on the hot ductility of TWIP and TRIP assisted steels: A critical review. *Metals* 2019; 12(502): 1–31. doi: 10.3390/met12030502.
43. Borrmann L., Senk D., Steenken B., Rezende J.L.L. Influence of cooling and strain rates on the hot ductility of high manganese steels within the system Fe-Mn-Al-C. *Steel Research* 2021; 92(2): 1–10. doi: 10.1002/srin.202000346.
44. Hutrtado-Delgado E., Morales R.D. Hot ductility and fracture mechanisms of a C-Mn-Nb-Al steel. *Metallurgical and Materials Transactions B* 2001; 32(5): 919–927. doi: 10.1007/s11663-001-0078-7.
45. Kaushik P., Lowry P., Yin H., Piolet H. Particles characterization for clean steelmaking and quality control. *Ironmaking & Steelmaking B* 2012; 39(4): 284–300. doi: 10.1179/1743281211Y.0000000069.
46. Liu H., Liu J., Michelic S.K., Wei W.F., Zhuang C., Li S.Q. Characteristic of AlN inclusions in low carbon Fe-Mn-Si-Al steel produced by AOD-ESR method. *Ironmaking & Steelmaking B* 2016; 43: 171–179. doi: 10.1179/1743281215Y.0000000028.
47. Kang S.E., Kang M.H., Mintz B. Influence of vanadium, boron and titanium on hot ductility of high Al TWIP steel. *Materials Science and Technology* 2020; 37(1): 42–58. doi: 10.1080/02670836. 2020.1861736.
48. Crowther D.N., Mintz B. Influence of grain size and precipitation of microalloyed steel. *Materials Science and Technology* 1986; 2(11): 1099–1105. doi: 10.1179/mst.1986.2.11.1099.
49. Fojt-Dymara G., Opiela M., Borek W. Susceptibility of high-manganese steel to high-temperature cracking. *Materials* 2022; 15(8198): 1–12. doi: 10.3390/ma15228198.

50. Qaban A., Mintz B., Kang S.E., Naher S. Hot ductility of high Al TWIP steels containing Nb and Nb-V. *Materials Science and Technology* 2017; 33: 1645–1656. doi: 10.1080/02670836.2017.1309097.
51. Osinkolu G.A., Tacikowski M., Kobylanski A. Combined effect of AlN and sulphur on hot ductility of high purity iron-base alloys. *Materials Science and Technology* 1985; 1: 520–525. doi: 10.1179/mst.1985.1.7.520.
52. Abushosha R., Ayyad S., Mintz B. Influence of cooling rate and MnS inclusions on the hot ductility of steels. *Materials Science and Technology* 1998; 14: 227–235. doi: 10.1179/mst.1998.14.3.227.
53. Kang S.E., Kang M.H., Mintz B. Influence of vanadium, boron and titanium on hot ductility of high Al, TWIP steels. *Materials Science and Technology* 2020; 37: 42–58. doi: 10.1080/02670836.2020.1861736.
54. Turkdogan E.T. Causes and effects of nitride and carbonitride precipitation during continuous casting. *Iron & Steelmaker* 1989; 16(5): 61–75.
55. Adrian H. Thermodynamic model for precipitation of carbonitrides in high strength low alloyed steels up to three microalloying elements with or without additions of aluminium. *Materials Science and Technology* 1992; 8: 406–420. doi: 10.1179/026708392790170991.
56. Opiela M. Thermodynamic analysis of precipitation process of MX-type phases in high strength low alloy steels. *Advances in Science and Technology. Research Journal* 2021; 15(2): 90–100. doi: 10.12913/22998624/135514.
57. Mintz B., Abushosha R. Effectiveness of hot tensile test in simulating straightening in continuous casting. *Materials Science and Technology* 1992; 8: 171–178. doi: 10.1179/mst.1992.8.2.171.
58. Grajcar A., Borek W. Thermo-mechanical processing of high-manganese austenitic TWIP-type steel. *Archives of Civil and Mechanical Engineering* 2008; 8(3): 29–38. doi: 10.1016/S1644-9665(12)60119-8.
59. Kuc D., Cebulski J. Plastic behavior and microstructure characterization high manganese aluminum alloyed steel for the automotive industry. *Journal of Achievements in Materials and Manufacturing Engineering* 2012; 51(1): 14–21.
60. Kawulok P., Schindler I., Navratil H., Sevcak H., Sojka J., Koncna K., Chmiel B. Hot formability of heat-resistance stainless steel X15CrNiSi20-12. *Archives of Metallurgy and Materials* 2019; 65(2): 727–734. doi: 10.24425/amm.2020.132812.